A method for measuring the soil radon emanation coefficient without disturbing the soil structure

Haoyu You[a]; Zhongkai Fan[a]; Ruomei Xie[a]; Hongzhi Yuan[a]; Yanliang Tan[a, *]

[a]College of Physics and Electronic Engineering, Hengyang Normal University,

[*]Corresponding author. E-mail address: hytyl@163.com

Abstract: Conventional measurements of the soil radon emanation coefficient often rely on drying, grinding, or repacking, which alters the native pore structure and moisture distribution of the sample. To obtain radon emanation coefficient that is more representative of natural soils, RAD7 was used to conduct closed-loop cumulative measurements on the intact in-situ soil samples. Soil samples without structural alteration were placed in an airtight acrylic accumulation chamber, and the radon concentration in the recirculating gas loop was recorded continuously for 24 h. The radon exhalation rate was determined by nonlinear fitting of the radon concentration variation curve, and the emanation coefficient was then calculated from the exhalation rate, sample dry mass, exposed area, and Ra-226 specific activity. Three natural soil samples were used to validate the method. All samples showed a typical nonlinear accumulation pattern, with rapid early growth followed by slower increase at later times, and the fitted R^2 values ranged from 0.86 to 0.92. The radon exhalation rates were 3.04 ± 0.35, 4.01 ± 0.34, and 4.69 ± 0.42 $mBq \cdot m^{-2} \cdot s^{-1}$, corresponding to emanation coefficients of 0.36 ± 0.04, 0.44 ± 0.04, and 0.59 ± 0.05, respectively. In the study, under the same specific activity of Ra-226, due to the differences in water content and porosity, different radon emanation coefficient were obtained. The proposed approach provides a practical basis for obtaining source-term parameters that are closer to actual field conditions for site screening, radon potential assessment, and foundation-soil evaluation.

Keywords: Radon emanation coefficient, Undisturbed soil, Radon exhalation rate, Closed-loop monitoring

1. Introduction

Rn-222 is a radioactive noble gas generated by the decay of Ra-226 in soils and rocks and transported upward through pore space toward the ground surface [1]. The World Health Organization identifies radon as a major indoor environmental carcinogen and treats its control as an important public-health task [2]. A systematic review of measurements in Chinese dwellings, schools, and offices also found strong spatial variation in indoor exposure levels [3]. Case-control data from Gansu further show that risk increases in high-exposure residential settings [4]. City-scale monitoring in Zhuhai already indicated that indoor radon is uneven even within one coastal urban area [5]. Because many low-rise buildings exchange air and soil gas across the foundation, the realism of any radon-risk assessment depends in part on how the ground source is characterized [1]. Methodological studies have therefore treated soil flux as a practical bridge between subsurface generation and exposure assessment [6]. Early national work demonstrated that soil exhalation data can be used to map broad radon-prone patterns across China [7]. The same line of research showed that soil texture and related physical properties influence both soil-gas concentration and surface release [8]. Later national-scale estimation confirmed that radon flux density in China is highly heterogeneous in space [9].

Radon exhalation rate is the outward expression of a deeper process, the key parameter is the fraction of radon atoms generated by Ra-226 that escape the solid phase into interconnected pore space [10]. Classic soil studies explicitly distinguish this radon emanation coefficient from surface exhalation rate [11]. Its value depends on recoil, diffusion, and phase partitioning at the grain scale rather than on boundary flux alone [12]. Reviews of radon migration therefore place emanation at the interface between radium occurrence in solids and subsequent transport in porous media [13]. Because the parameter separates release efficiency from simple source inventory, it underpins geogenic radon mapping and source-strength comparison [14]. In this sense, the emanation coefficient is the parameter that links soil physical state to the exhalation eventually observed at the surface [10]. Field measurements from Chinese sedimentary and granite terrains illustrate that soils with broadly comparable geological settings can still yield different exhalation intensities [15]. Surveys in high-background areas of South China likewise show that subsurface radon occurrence is strongly site dependent [16]. Urban observations in Shenzhen further indicate that soil-gas radon and thoron respond sensitively to local near-surface conditions [17]. Recent work in Urumqi has extended this point by linking indoor and soil-gas radon characteristics to regional radon potential [18].

Previous studies agree that the radon emanation coefficient is not a fixed material label,

because it changes with geological setting and climatic state [19]. Controlled chamber experiments showed early on that soil moisture can alter emanation substantially even when the solid source remains unchanged [20]. Japanese experiments later clarified the nonlinearity of this response by showing that radon and thoron release vary strongly with water content [21]. Measurements on representative Okinawan soils likewise confirmed that natural soils span a broad range of emanation coefficients [22]. More recent experiments have added grain size, porosity, and mineralogical controls to this picture by linking soil characteristics to both emanation and diffusion [23]. A factor analysis by researchers concluded that moisture, temperature, porosity, mineral composition, and radium occurrence mode act together rather than independently [24]. This coupling means that single-factor interpretation is often unstable unless the structural state of the sample is clearly defined [24]. Heating experiments on loess further showed that thermally induced structural change can shift the release behavior of the same material [25]. Depth-resolved measurements in northern Shaanxi then indicated that lithology and burial context also modify radon release patterns [26]. Work focused on loess moisture demonstrated again that water content can reorganize emission behavior over a realistic field range [27].

At a broader scale, recent compilation and upscaling work emphasized that radon-flux data still reflect strong methodological and environmental heterogeneity [28]. Fault-zone studies in Beijing demonstrated that soil-gas radon can respond sharply to structurally controlled degassing pathways [29]. Similar evidence from Tangshan connected soil-gas radon anomalies with the activity of seismogenic faults [30]. Measurements across the Anninghe and Zemuhe fault systems reached a comparable conclusion for southwestern China [31]. Degassing research along the western Ordos margin likewise showed that active structures modulate radon transfer from depth to the near surface [32]. Even outside obvious fault belts, basin-scale surveys in Gansu recorded pronounced variability in soil-gas radon [33]. Karst investigations in southwest China further suggested that special pore-fracture systems can generate localized soil-radon anomalies [34]. These observations help explain why some researchers have tried to estimate emanation and diffusion coefficients simultaneously rather than treat release as a simple constant [35]. In parallel, one-cycle chamber analysis was proposed to accelerate exhalation measurement under controlled conditions [36]. Ventilation-type accumulation procedures were then introduced to trace concentration growth more efficiently [37]. Open-loop calculation frameworks were also revised to reduce bias from nonideal accumulation behavior [38]. Closed-chamber studies further improved quantitative treatment of exhalation through tighter mass-balance analysis and calibration [39]. Reference-device comparisons with AlphaGUARD confirm that

measurement mode and circuit configuration still affect the derived result [40]. Recent instrument development has improved continuous in situ monitoring of soil radon in fault zones [41].

The review literature shows that methodological discussion has centered more on measurement procedure than on structural representativeness of the tested soil [10]. In many laboratory workflows, soils are dried, crushed, sieved, or repacked before testing because those operations simplify geometry and reduce measurement difficulty [10]. The practical difficulty is that emanation is controlled by micro-scale release, whereas most experiments observe radon only after it has already crossed a chamber-scale boundary [13]. Any pretreatment step that changes the route between recoil site and accessible pore can therefore alter the measured coefficient even when Ra-226 activity remains unchanged [12]. Drying is especially sensitive because it redistributes water films that may enhance recoil capture at low saturation but hinder further transfer at higher saturation [21]. Crushing and sieving can expose fresh mineral surfaces while simultaneously destroying the original pore network through which radon had migrated in the field [23]. Repacking then creates a second artificial structure defined by laboratory handling rather than by the natural soil state [24]. Such pretreatment can reorganize pore characteristics and moisture-bearing microenvironments that are already known to influence radon release [42]. A coefficient obtained from disturbed material may therefore describe a reconstructed medium rather than the current release efficiency of the original soil body [43]. This is a fundamental reason why values from prepared samples are difficult to transfer directly into near-surface transport models or building-site assessments [14].

Field systems can preserve environmental context more effectively, but current in situ instruments mainly target soil-gas monitoring rather than direct derivation of an emanation coefficient for an intact sample [41]. A method that preserves native geometry while keeping chamber mass balance manageable is therefore still needed [39]. Otherwise, improved precision may only refine the behavior of an artificial sample rather than reveal the behavior of the soil in place [14]. That distinction is crucial when emanation data are used as input to transport models and risk screening [13]. This unresolved problem motivates the present study. Here we collect soil with a stainless-steel ring cutter to preserve the existing structure as much as possible, and we measure the radon emanation coefficient on relatively intact samples instead of fully disturbed and repacked material. This strategy is intended to retain the real arrangement of particles, pores, and moisture-bearing microenvironments that control radon release more faithfully than conventional pretreatment. By providing a coefficient that is closer to the present structural state of the soil, the method should offer a more realistic basis

for source-strength evaluation, radon transport modeling, and radon-risk assessment for building sites. The objective of this study is to test and demonstrate the feasibility and significance of measuring soil radon emanation coefficients with ring-cutter intact sampling.

2. Materials and Methods

2.1 Experimental equipment and preparation

The experimental site was located on an unpaved natural ground surface in Hengyang, Hunan Province. Because the sensitivity of the RAD7 decreases markedly under high-humidity conditions, the surface soil at candidate points was first rapidly screened with a digital soil-moisture meter before sampling, and areas with extremely high moisture were excluded. Soil samples with unaltered soil structure were collected by slowly and uniformly pressing a stainless-steel ring cutter with an inner diameter of 10 cm and a height of 8 cm into the soil, corresponding to a sample volume of 500 cm^3. This size provides sufficient radioactivity by counting statistics while minimizing disturbance to the natural pore connectivity during sampling. After retrieval, the bottom of the ring cutter was immediately sealed and the sample was transported back to the laboratory, where it was left undisturbed for 48 h at ambient temperature to allow sampling stress release and short-term gas exchange to stabilize. No drying, crushing, or recompaction treatment was applied to the samples during the entire RAD7 monitoring stage.

The advantage of ring-cutter sampling is that the geometric boundaries of the sample are clearly defined, which facilitates incorporation of exposed area, sample volume, and dry mass into a unified calculation framework. Compared with collecting bulk soil and then repacking it into a container, ring-cutter samples do not require secondary compaction or leveling during transport and installation, thereby reducing opportunities for artificial reconstruction of the pore structure. For soils under natural conditions, this integrated preservation of geometry and structure is more important than simply increasing the number of samples, because the emanation coefficient corresponds to the efficiency of radon release from the soil body in its existing structural state rather than to the characteristic value of a fully homogenized material.

The measurement system consisted of an airtight acrylic accumulation chamber, a recirculating gas circuit, a miniature pump, a drying tube, a Nafion tube, temperature and humidity sensors, and a RAD7 electronic radon detector. A fixed effective gas-phase space was set above the accumulation chamber. The circulation pump drove chamber gas through drying and dehumidification into the RAD7 and then back to the chamber, forming a closed-loop circulation. Unlike a simple static end-point measurement, the closed-loop system can continuously record the concentration growth process without opening the chamber,

thereby preserving both early-stage growth information and late-stage decay constraints. The RAD7 was operated in sniff mode, using only the Po-218 signal to infer the Rn-222 concentration, so as to improve the response speed to concentration changes. The instrument was calibrated in the national standard radon chamber at the University of South China, and the calibration factor for Rn-222 detection was 1.17. During formal measurements, a single sampling cycle was set to 60 min and was repeated continuously for 24 cycles, giving a total monitoring duration of 24 h.

To ensure comparability among different samples, this study kept the sample geometry, exposed area, and closed-loop gas-circuit configuration identical. The accumulation chamber and connecting pipelines were checked for airtightness before each experiment, and connecting tubes of the same length, the same model of drying tube, and the same circulation flow setting were used to avoid additional bias caused by geometric differences in the apparatus. Because the RAD7 is sensitive to humidity, the Nafion tube in the closed loop not only lowered the humidity to the operating range of the instrument but also helped reduce the total volume of the closed-loop system.

Figure 1 shows the natural-state measurement apparatus used in this study. By combining unaltered soil structure samples with closed-loop dynamic monitoring, it provided a complete time series for subsequent full-process nonlinear fitting.

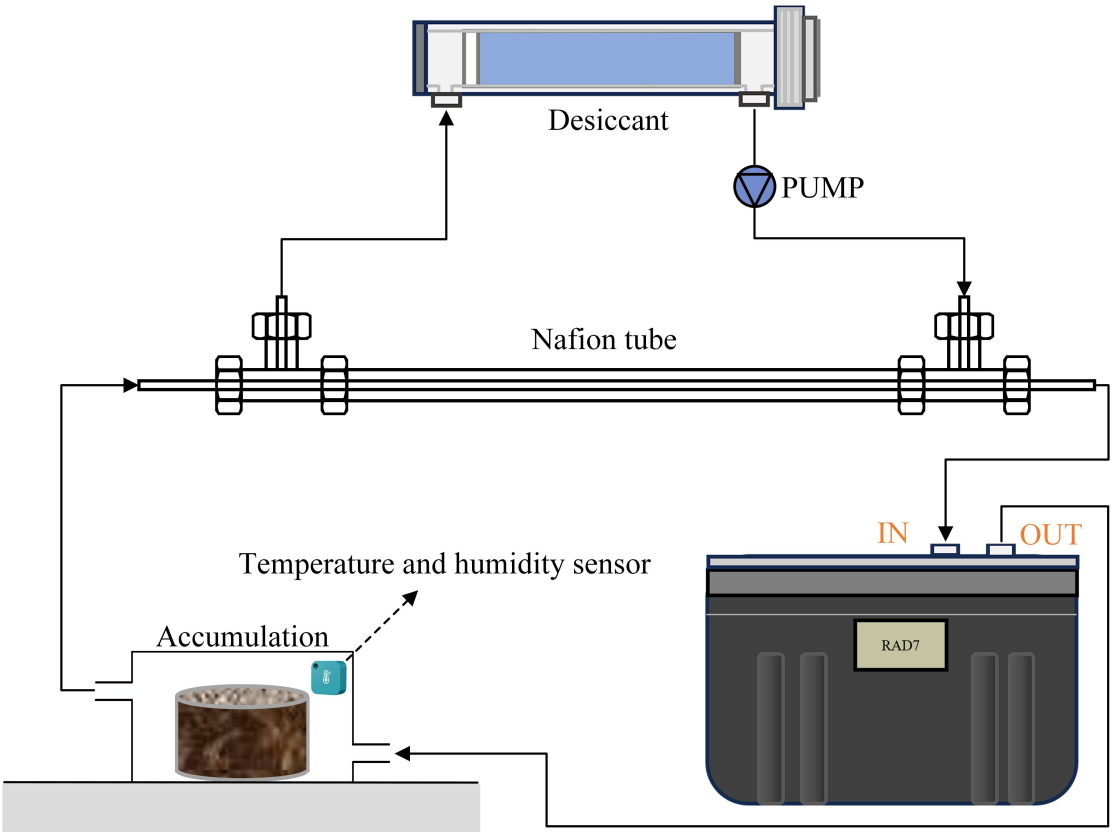

Figure 1. Schematic diagram of the apparatus for measuring the soil radon emanation

coefficient

2.2 Formula Derivation and Data Processing

In soil, Ra-226 undergoes alpha decay to produce Rn-222. If the radon emanation coefficient is denoted by e, the temporal change in radon activity within soil particles can be written as Eq. (1).

$$\frac{dA_{Rn}(t)}{dt} = A_{Ra}\lambda_{Rn}(1-e) - A_{Rn}(t)\lambda_{Rn} \tag{1}$$

where A_{Rn} is the Rn-222 activity in the soil solid phase, A_{Ra} is the Ra-226 activity, and lambda is the decay constant of Rn-222.

When Ra-226 and Rn-222 reach dynamic equilibrium within the particles, Eq. (2) is obtained.

$$\frac{dA_{Rn}(t)}{dt} = 0 \tag{2}$$

From the dynamic equilibrium relationship, the expression for releasable radon in the pore space can be obtained and further written as the emanation-coefficient equation, Eq. (3).

$$e = \frac{A_{Ra} - A_{Rn}}{A_{Ra}} = \frac{A'_{Rn}}{A_{Ra}} \tag{3}$$

In an airtight accumulation chamber, if the radon exhalation rate from the soil surface is J, the exposed surface area is S, and the effective gas-phase volume of the closed loop is V, then the chamber concentration growth process under continuous exhalation and radioactive decay can be described by Eq. (4). All 24 time-series concentration values obtained by the RAD7 were imported into Origin 2024, and Eq. (4) was fitted by nonlinear least squares to obtain J. Compared with methods that use only the linear slope at the initial stage of accumulation, full-process fitting can substantially reduce the amplification of random fluctuations in the first few data points.

$$C_{Rn}(t) = C_{po}(t) = \frac{JS\left[\lambda_e\left(1-e^{-\lambda_{po}t}\right) - \lambda_{po}\left(1-e^{-\lambda_e t}\right)\right]}{\lambda_e V(\lambda_e - \lambda_{po})} \tag{4}$$

After completion of RAD7 dynamic monitoring, porosity was measured by the volume displacement method. Keeping the ring cutter and the undisturbed soil sample level, purified water was slowly injected until the sample was fully saturated, and the injected water volume was recorded. The porosity was then calculated according to Eq. (5). Because this step was arranged after the radon exhalation experiment, it did not additionally interfere with the original measurements during the radon release stage.

$$\eta = \frac{V_w}{V_T} \times 100\% \tag{5}$$

where V_T is the total sample volume, i.e., the volume of the ring cutter, and V_w is the volume of water required to reach saturation. The dry mass m of the sample was obtained by the constant-weight method.

The sample was placed in a stainless-steel tray and dried continuously for 6 h in a constant-temperature oven at 200 ± 5 °C. After cooling to room temperature, it was weighed, and the drying and weighing procedures were repeated until the difference between two consecutive measurements met the constant-weight criterion.

The Ra-226 specific activity a_{Ra} was measured using a CIT3000F low-background gamma spectrometry system. After RAD7 monitoring, the samples were dried, ground, and passed through a 0.1 mm sieve. Then 500.0 ± 0.1 g of each sample was weighed into a polyethylene sample box, sealed, and left for more than 25 d at 20 ± 1 °C to ensure radioactive equilibrium between Rn-222 and its progeny and Ra-226. Counting was performed for 4 h in a lead-shielded chamber with a thickness of 10 cm, and the Ra-226 specific activity was converted from the area of the characteristic energy peak. Using the measured values of J, S, m, and a_{Ra}, the soil radon emanation coefficient e was calculated according to Eq. (6).

$$e = \frac{J \cdot S}{a_{Ra} \cdot m \cdot \lambda_{Rn}} \tag{6}$$

where e is the dimensionless radon emanation coefficient; S is the exposed surface area; J is the radon exhalation rate; m is the dry mass of the sample; a_{Ra} is the specific activity of Ra-226; and λ_{Rn} is the decay constant of Rn-222. Because the Ra-226 specific activities of the three sample groups in this study were similar, the independent effects of pore structure and moisture distribution on the emanation coefficient could be identified more clearly. The result will consider the fitting R^2, the overall shape of the concentration growth curve, and the consistency of parameter trends.

3. Results

The physical parameters of the three soil samples with unaltered soil structure are

summarized in Table 1. The masses were 645.5 g for Sample 1; 686.2 g for Sample 2; and 625.7 g for Sample 3, and the volume of each sample was 500 cm^3. The porosity values were 19.1% for Sample 1; 18.2% for Sample 2; and 26.4% for Sample 3, whereas the moisture contents were 16.3% for Sample 1; 19.6% for Sample 2; and 23.7% for Sample 3. Sample 3 showed the highest porosity and moisture content, indicating a relatively loose solid skeleton and greater retention of natural moisture in the pores. Samples 1 and 2 had similar porosity, but their moisture contents were clearly different and this makes them suitable for analyzing the moisture effect within the intermediate moisture range. The Ra-226 specific activities were 48.93 $Bq \cdot kg^{-1}$ for Sample 1; 48.86 $Bq \cdot kg^{-1}$ for Sample 2; and 47.09 $Bq \cdot kg^{-1}$ for Sample 3, with a maximum relative difference of only 3.76%. This indicates that the subsequent differences in radon accumulation were not mainly controlled by source strength.

Because the three groups of samples had similar source strengths but different structures and moisture conditions, the experiment effectively created an ideal natural-state comparison scenario. In other words, if the different samples ultimately exhibited significantly different radon exhalation rates and emanation coefficients, such differences were more likely attributable to the physical state of the soil rather than to the Ra-226 content itself.

The 24 h radon concentration time series obtained by continuous RAD7 monitoring are shown in Table 2. All three samples exhibited an accumulation trend that was rapid at first and then slowed, and a gradual approach to equilibrium appeared at later times, indicating that the closed-loop system successfully captured the typical nonlinear growth process jointly controlled by continuous exhalation and radioactive decay. For Sample 1, the concentration increased from 107.76 $Bq \bullet m^{-3}$ at 1800 s to 525.35 $Bq \bullet m^{-3}$ at 77400 s; for Sample 2, from 140.53 $Bq \bullet m^{-3}$ to 610.98 $Bq \bullet m^{-3}$; and for Sample 3, from 167.45 $Bq \bullet m^{-3}$ to 742.10 $Bq \bullet m^{-3}$. Although local declines occurred in a few periods in the middle and later stages, such as around 23400 s for Sample 1 and around 27000 s for Sample 3, these statistical fluctuations did not affect the overall parameter trends.

Table 2. Radon concentrations monitored by RAD7 during the 24 h accumulation process for the three sample groups

Time (s)	Sample 1 Radon concentration ($Bq \bullet m^{-3}$)	Sample 2 Radon concentration ($Bq \bullet m^{-3}$)	Sample 3 Radon concentration ($Bq \bullet m^{-3}$)
1800	107.76±44.96	140.53±48.06	167.45±53.17
5400	116.42±52.51	205.26±56.86	237.15±64.18
9000	147.59±60.12	255.88±66.71	279.78±73.18
12600	178.89±66.31	278.37±73.81	324.28±81.38

16200	255.67±76.42	320.55±76.54	360.94±84.65
19800	292.60±83.17	340.23±80.44	384.19±91.63
23400	227.66±82.08	331.80±85.15	449.64±99.39
27000	333.72±91.95	441.65±92.42	407.14±98.74
30600	333.87±93.08	444.47±92.24	567.09±111.10
34200	401.20±100.51	441.65±91.51	468.72±109.52
37800	342.29±99.17	447.28±94.94	451.68±110.90
41400	331.06±101.82	478.44±97.60	525.54±115.26
45000	451.91±106.19	551.61±102.96	534.06±117.59
48600	384.54±107.90	560.05±101.65	636.33±121.42
52200	356.47±107.90	492.29±99.77	582.62±121.48
55800	392.96±111.24	500.95±101.48	676.40±129.70
59400	480.19±116.53	574.12±105.21	622.40±125.32
63000	437.87±115.05	540.35±105.21	665.03±130.22
66600	404.37±115.10	531.91±105.84	611.04±129.04
70200	390.15±113.45	495.32±105.21	574.35±132.72
73800	376.29±115.67	591.27±109.77	624.69±131.52
77400	525.35±125.60	610.98±107.93	742.10±139.17
81000	505.46±121.67	500.95±102.79	656.80±135.86
84600	435.26±121.67	571.56±109.77	597.09±132.59

Figure 2 presents the fitting results corresponding to the three time series. All three fitted curves passed through the main distribution range of the measured points, and both the early-stage slope and the late-stage quasi-equilibrium features were reproduced well, indicating that the mass-balance model based on Eq. (4) can reasonably describe the radon accumulation process in the closed-loop system used in this study. This is particularly important for soil samples with unaltered soil structure, because the structural heterogeneity of natural samples often produces more pronounced statistical fluctuations within a single sampling cycle; if only the first few points are used to calculate the slope, short-term fluctuations can easily be misidentified as differences in exhalation rate.

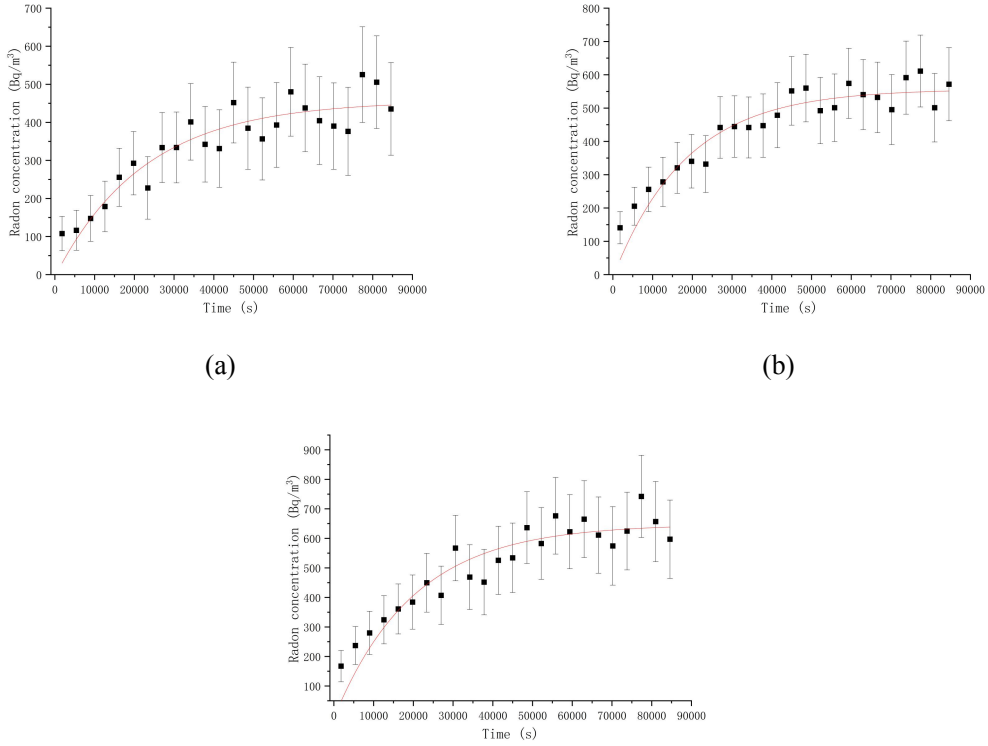

Figure 2. Fitted radon concentration curves for the three samples, 2-(a), 2(b), and 2-(c) represent Sample 1, Sample 2, and Sample 3, respectively

Table 3 summarizes the fitted radon exhalation rates and emanation coefficients. The radon exhalation rates of Samples 1, 2, and 3 were 3.04 ± 0.35, 4.01 ± 0.34, and 4.69 ± 0.42 $mBq \cdot m^{-2} \cdot s^{-1}$, respectively; the fitted R^2 values were 0.86, 0.92, and 0.90, respectively; and the corresponding emanation coefficients were 0.36 ± 0.04, 0.44 ± 0.04, and 0.59 ± 0.05, respectively. Compared with Sample 1, Sample 3 showed a 54.28% increase in radon exhalation rate and a 63.89% increase in emanation coefficient, indicating that under the combined action of high porosity and high moisture content, more recoil radon can enter the mobile pore space from the solid phase. Although the porosity of Sample 2 was slightly lower than that of Sample 1, its moisture content was higher, and its emanation coefficient still increased from 0.36 to 0.44, indicating that within the natural moisture range of this study, the moisture effect was not offset by small structural differences.

Table 3. Radon exhalation rates and emanation coefficients of the samples

Parameter	Radon exhalation rate ($mBq \cdot m^{-2} \cdot s^{-1}$)	R^2	Emanation coefficient
Sample 1	3.04±0.35	0.86	0.36±0.04
Sample 2	4.01±0.34	0.92	0.44±0.04
Sample 3	4.69±0.42	0.90	0.59±0.05

It is worth noting that the 24 h monitoring duration of the three samples was much

shorter than the full half-life of Rn-222, and therefore the measured curves did not truly reach the ultimate equilibrium concentration in the strict sense. However, because Eq. (4) simultaneously incorporates the continuous source term and the decay constraint, the fitting still yielded stable exhalation-rate estimates. The low-to-high ranking of the parameters among the different samples was entirely consistent with the trends in moisture content and porosity, and this internal consistency strengthens the credibility of the results.

From the perspective of combined parameter relationships, the comparison between Samples 1 and 2 best reflects the independent role of moisture, because their porosities are similar whereas their moisture contents differ; the comparison between Samples 2 and 3 more strongly reflects the superimposed enhancement of pore structure and moisture. In other words, within the ranges of sample moisture content and porosity in this study, the thin-water-film effect associated with increasing moisture content first promoted an increase in the emanation coefficient, and when porosity further increased, this growth was additionally amplified by better gas-phase connectivity.

4. Discussion

The emanation coefficients of 0.36-0.59 obtained in this study are overall higher than the representative soil value of 0.20 commonly cited in the review by Sakoda et al. [10], but they are not inconsistent with the observations of Markkanen and Arvela, Sun and Furbish, and Bossew that moderate moisture contents can significantly enhance emanation capacity [11,44,45]. Hosoda et al. found in experiments on radon and thoron emanation from soil that increasing moisture content first promotes and then suppresses gas release [21]. Huynh et al. further pointed out that for soils with different particle-size fractions, the emanation coefficient can rapidly approach a stable high value within a certain moisture range [23]. The moisture contents of the three samples in this study were concentrated between 16.3% and 23.7%, which lies precisely within the range where thin water films promote the escape of recoil radon while the pores are not yet excessively blocked by water, and thus the relatively high yet reasonable emanation coefficients obtained here have a clear physical basis.

From the perspective of medium structure, the results of this study are also mutually corroborative with existing knowledge on different soils and fractured media in China. Studies of soils with different lithologies in northern Shaanxi and the pore structures of coal in northern China have shown that the proportion of micropores, contact relationships among mineral particles, and weathering features related to depth jointly alter radon release pathways [26,46]. Results for thermally treated loess indicate that particle-surface conditions and pore reorganization can significantly rearrange exhalation rates [25]. Two-dimensional fracture

models and fractal discrete fracture network models further show that once fracture connectivity is enhanced, radon migration flux can be further amplified [47,48]. Sample 3 in the present study had both the highest porosity and the highest moisture content, and therefore ranked highest among the three in all parameters, which is consistent with the structural control mechanisms described above.

This undisturbed-soil measurement strategy also has direct implications for engineering practice. Regional radon potential assessment often requires rapid comparisons across a large number of sites, whereas radon-protection design for building sites requires parameters that are as close as possible to actual foundation-soil conditions. If standard parameters obtained from dried and reconstructed samples are used, laboratory repeatability may be improved, but the true release capacity of natural soils with moderate moisture content may be underestimated. Conversely, if one relies entirely on instantaneous in situ soil-gas concentration, the results are easily affected by meteorological conditions and boundary disturbances. The method proposed here lies between these two approaches: it preserves the repeatability of controlled indoor measurements while establishing a more direct connection between the results and the natural field structure.

The potential application scenarios of the present method are not limited to ordinary site soils. Studies of the temperature dependence of the radon diffusion coefficient in porous media have shown that once transport parameters are coupled with temperature and humidity, empirical values obtained under a single standard condition become difficult to extrapolate [49]. In studies of heap-leached uranium ore columns, red-clay-bentonite cover layers, and anomalous radon sources in underground spaces, researchers have likewise found that small changes in material structure, moisture boundary, and source occurrence state may lead to significant shifts in exhalation behavior [50,51,52]. The latest work on the occurrence modes of U and Ra in sandstone-type uranium ores further indicates that, even under similar source strengths, differences in the distribution positions of radionuclides within mineral particles can feed back on radon release efficiency [53].

Furthermore, the environmental interpretation of the emanation coefficient cannot be separated from scale conditions. At the macroscopic site scale, the actual migration of radon from soil to indoor space is also controlled by foundation cracks, pressure differences, surface cover, and seasonal changes in moisture. Therefore, the parameters obtained in this study cannot be mechanically equated with indoor radon concentration itself. Nevertheless, at the level of source identification, site screening, and relative comparison among different soils, the emanation coefficient obtained after preserving the undisturbed structure remains irreplaceably valuable, because it provides a more robust input parameter for linking indoor

intrusion models with the actual radon exhalation capacity of soils.

Measurements on soil with unaltered soil structure can also improve the interpretability of parameter comparisons among different sites. If the method proposed here is combined in the future with standardized sampling depth, unified indoor/outdoor environmental records, and GIS-based geological-unit databases, it will be possible to build spatial distribution maps of the emanation coefficient that remain experimentally repeatable while being closer to actual surface conditions. Such databases could serve not only for identifying high-radon areas, but also for providing more refined source-term inputs for underground-space development, ventilation design of underground engineering works, and performance evaluation of ecological cover layers.

The comparison of three sample groups with similar Ra-226 specific activities in this study has another important implication: it demonstrates that even when source-strength differences are compressed, the method can still stably resolve differences in radon release. In many site investigations, the most difficult question is not whether the soil contains radium, but which locations are more prone to supplying radon upward under similar source-term backgrounds. Although the number of samples in this study was limited, the results show that variations in moisture content and porosity are sufficient to cause significantly different emanation coefficients, which means that the discriminative sensitivity of this method has practical value for engineering screening.

This study still belongs to methodological validation and preliminary application. Although the undisturbed structure was maintained during the sampling and monitoring stages, particle-size distributions, mineral composition, specific surface area, and in situ soil-gas profile data were not obtained simultaneously, and thus the relative contributions of moisture content, porosity, and mineralogical factors could not be quantitatively separated. Although 24 h monitoring is sufficient to support exhalation-rate fitting, longer time series and more replicate samples are still required to test stability for lower-activity samples or under seasonal freezing-drying-wetting cycles. Future work should therefore carry out repeated experiments across more soil types, more seasons, and wider moisture gradients, and should integrate analyses within situ soil-gas flux, indoor intrusion risk, and regional radon potential assessment, to establish a practical parameter database that balances realism, repeatability, and engineering utility.

5. Conclusions

This study presents a practical method for estimating the radon emanation coefficient of

natural-state soils while preserving their original structure and moisture distribution. By combining ring-cutter intact sampling, closed-loop RAD7 monitoring, and full-curve nonlinear fitting, the method reduces the bias introduced by drying, crushing, and repacking and therefore yields parameters that are closer to actual near-surface soil conditions.

For the three soil samples with similar Ra-226 specific activities, the 24 h concentration curves were described satisfactorily by the accumulation model, with fitted R^2 values of 0.86-0.92. The corresponding radon exhalation rates were 3.04 ± 0.35, 4.01 ± 0.34, and 4.69 ± 0.42 mBq·m^{-2}·s^{-1}, and the emanation coefficients were 0.36 ± 0.04, 0.44 ± 0.04, and 0.59 ± 0.05, respectively. Under comparable source-strength conditions, both parameters increased from Sample 1 to Sample 3, indicating that higher moisture content and greater pore connectivity enhanced radon release efficiency in the tested natural soils.

These results show that preserving the undisturbed state of the soil is important when the goal is to evaluate relative release capability rather than the behavior of an artificially reconstructed sample. The proposed method is therefore suitable for site screening, comparison of natural soils, and provision of source-term parameters for radon potential assessment and foundation-soil evaluation. Because the present work remains a preliminary validation based on a limited number of samples, further testing across more soil types, moisture ranges, and seasonal conditions are still needed before broader empirical relationships are established.

References

[1] W. W. Nazaroff, Radon transport from soil to air, Reviews of Geophysics 30(2), 137 – 160 (1992), doi:10.1029/92RG00055.

[2] World Health Organization, Ed., WHO handbook on indoor radon: a public health perspective, World Health Organization, Geneva, Switzerland (2009).

[3] C. Su et al., Indoor exposure levels of radon in dwellings, schools, and offices in China from 2000 to 2020: A systematic review, Indoor Air 32(1) (2022), doi:10.1111/ina.12920.

[4] Z. Wang, Residential Radon and Lung Cancer Risk in a High-exposure Area of Gansu Province, China, American Journal of Epidemiology 155(6), 554 – 564 (2002), doi:10.1093/aje/155.6.554.

[5] C. Diyun, Y. Xingbao, and H. Ruiying, Indoor radon survey in indoor environments in Zhuhai city, China, Radiation Measurements 39(2), 205 – 207 (2005), doi:10.1016/j.radmeas.2004.04.012.

[6] Q. Guo, Methodology study on evaluation of radon flux from soil in China, Radiation

Protection Dosimetry 112(2), 291 – 296 (2004), doi:10.1093/rpd/nch387.

[7] K. Sun, Q. Guo, and W. Zhuo, Feasibility for Mapping Radon Exhalation Rate from Soil in China, Journal of Nuclear Science and Technology 41(1), 86 – 90 (2004), doi:10.1080/18811248.2004.9715462.

[8] K. Sun, Q. Guo, and J. Cheng, The Effect of Some Soil Characteristics on Soil Radon Concentration and Radon Exhalation from Soil Surface, Journal of Nuclear Science and Technology 41(11), 1113 – 1117 (2004), doi:10.1080/18811248.2004.9726337.

[9] W. Zhuo et al., Estimating the amount and distribution of radon flux density from the soil surface in China, Journal of Environmental Radioactivity 99(7), 1143 – 1148 (2008), doi:10.1016/j.jenvrad.2008.01.011.

[10] Sakoda, Y. Ishimori, and K. Yamaoka, A comprehensive review of radon emanation measurements for mineral, rock, soil, mill tailing and fly ash, Applied Radiation and Isotopes 69(10), 1422 – 1435 (2011), doi:10.1016/j.apradiso.2011.06.009.

[11] M. Markkanen and H. Arvela, Radon Emanation from Soils, Radiation Protection Dosimetry 45(1 – 4), 269 – 272 (1992), doi:10.1093/rpd/45.1-4.269.

[12] V. C. Rogers and K. K. Nielson, Multiphase Radon Generation and Transport in Porous Materials:, Health Physics 60(6), 807 – 815 (1991), doi:10.1097/00004032-199106000-00006.

[13] N. M. Hassan et al., Radon Migration Process and Its Influence Factors; Review, Hoken Butsuri 44(2), 218 – 231 (2009), doi:10.5453/jhps.44.218.

[14] J. Kemski et al., Mapping the geogenic radon potential in Germany, Science of The Total Environment 272(1 – 3), 217 – 230 (2001), doi:10.1016/S0048-9697(01)00696-9.

[15] N. Wang et al., Level of Radon Exhalation Rate from Soil in Some Sedimentary and Granite Areas in China, Journal of Nuclear Science and Technology 46(3), 303 – 309 (2009), doi:10.1080/18811248.2007.9711534.

[16] N. Wang et al., Distribution and Characteristics of Radon Gas in Soil from a High-Background-Radiation City in China, Journal of Nuclear Science and Technology 48(5), 751 – 758 (2011), doi:10.1080/18811248.2011.9711758.

[17] N. Wang et al., The characteristics of radon and thoron concentration from soil gas in Shenzhen City of Southern China, Nukleonika 61(3), 315 – 319 (2016), doi:10.1515/nuka-2016-0052.

[18] N. Wang et al., Characteristics of Indoor and Soil Gas Radon, and Discussion on High Radon Potential in Urumqi, Xinjiang, NW China, Atmosphere 14(10), 1548 (2023), doi:10.3390/atmos14101548.

[19] R. R. Schumann and L. C. S. Gundersen, Geologic and climatic controls on the radon

emanation coefficient, Environment International 22, 439 – 446 (1996), doi:10.1016/S0160-4120(96)00144-4.

[20] M. Y. Menetrez et al., Evaluation of radon emanation from soil with varying moisture content in a soil chamber, Environment International 22, 447 – 453 (1996), doi:10.1016/S0160-4120(96)00145-6.

[21] M. Hosoda et al., Effect of Soil Moisture Content on Radon and Thoron Exhalation, Journal of Nuclear Science and Technology 44(4), 664 – 672 (2007), doi:10.1080/18811248.2007.9711855.

[22] Y. Shiroma et al., Estimation of radon emanation coefficient for representative soils in Okinawa, Japan, Radiation Protection Dosimetry 167(1 – 3), 147 – 150 (2015), doi:10.1093/rpd/ncv233.

[23] H. N. Phong Thu, N. Van Thang, and L. C. Hao, The effects of some soil characteristics on radon emanation and diffusion, Journal of Environmental Radioactivity 216, 106189 (2020), doi:10.1016/j.jenvrad.2020.106189.

[24] W. Zhang, Y. Zhang, and Q. Sun, Analyses of Influencing Factors for Radon Emanation and Exhalation in Soil, Water Air Soil Pollut 230(1), 16 (2019), doi:10.1007/s11270-018-4063-z.

[25] P. Li et al., Radon exhalation from temperature treated loess, Science of The Total Environment 832, 154925 (2022), doi:10.1016/j.scitotenv.2022.154925.

[26] P. Li et al., A study on the differences in radon exhalation of different lithologies at various depths and the factors influencing its distribution in northern Shaanxi, China, Science of The Total Environment 849, 157935 (2022), doi:10.1016/j.scitotenv.2022.157935.

[27] J. Luo, Study on the influence of water content on radon emission from loess, Journal of Environmental Radioactivity 273, 107371 (2024), doi:10.1016/j.jenvrad.2024.107371.

[28] B. Lei et al., Overview and large-scale representative estimate of radon-222 flux data in China, Environmental Advances 11, 100312 (2023), doi:10.1016/j.envadv.2022.100312.

[29] Z. Chen et al., Radon emission from soil gases in the active fault zones in the Capital of China and its environmental effects, Sci Rep 8(1), 16772 (2018), doi:10.1038/s41598-018-35262-1.

[30] X. Wang et al., Correlations between radon in soil gas and the activity of seismogenic faults in the Tangshan area, North China, Radiation Measurements 60, 8 – 14 (2014), doi:10.1016/j.radmeas.2013.11.001.

[31] Y. Yang et al., Correlations between the radon concentrations in soil gas and the activity of the Anninghe and the Zemuhe faults in Sichuan, southwestern of China, Applied

Geochemistry 89, 23 – 33 (2018), doi:10.1016/j.apgeochem.2017.11.006.

[32] Z. Liu et al., Degassing of soil gas radon and its implication to fault activity in the western margin of the Ordos Block, China, Terra Nova 36(3), 191 – 200 (2024), doi:10.1111/ter.12695.

[33] B. Lei et al., Investigation on the soil gas radon concentrations in Northwest Huahai Basin, Gansu Province, China, J Radioanal Nucl Chem 326(1), 1 – 9 (2020), doi:10.1007/s10967-020-07280-9.

[34] Q. Ma et al., A preliminary study on soil radon anomaly and its formation mechanism in karst area of southwest China, J Radioanal Nucl Chem 331(5), 2045 – 2054 (2022), doi:10.1007/s10967-022-08259-4.

[35] N. K. Ryzhakova, A new method for estimating the coefficients of diffusion and emanation of radon in the soil, Journal of Environmental Radioactivity 135, 63 – 66 (2014), doi:10.1016/j.jenvrad.2014.04.002.

[36] Y. Tan and D. Xiao, A novel method to measure the radon exhalation rate in only one measurement cycle, Anal. Methods 5(3), 805 – 808 (2013), doi:10.1039/C2AY26134K.

[37] Y. Tan et al., Measuring radon exhalation rate by tracing the radon concentration of ventilation-type accumulation chamber, Radiation Measurements 58, 33 – 36 (2013), doi:10.1016/j.radmeas.2013.07.011.

[38] Y. Tan et al., Revision for measuring radon exhalation rate in open loop, J. Inst. 8(01), T01004 – T01004 (2013), doi:10.1088/1748-0221/8/01/T01004.

[39] L. Zhang et al., Accurate measurement of the radon exhalation rate of building materials using the closed chamber method, J. Radiol. Prot. 32(3), 315 – 323 (2012), doi:10.1088/0952-4746/32/3/315.

[40] S. Liu et al., COMPARISON OF RADON EXHALATION RATE MEASUREMENTS ON REFERENCE DEVICE IN OPEN AND CLOSED LOOP BY ALPHAGUARD IN FLOW-THROUGH MODE, Radiation Protection Dosimetry 199(10), 1151 – 1157 (2023), doi:10.1093/rpd/ncad063.

[41] Y. Zhao et al., Applied experimental research on in-situ online monitoring instrument for soil radon in fault zone, Journal of Environmental Radioactivity 280, 107546 (2024), doi:10.1016/j.jenvrad.2024.107546.

[42] F. Jiang et al., Experimental study of pore characteristics and radon exhalation of uranium tailing solidified bodies in acidic environments, Environ Sci Pollut Res 28(16), 20111 – 20120 (2021), doi:10.1007/s11356-020-12039-6.

[43] C. Huang et al., Variation rules of the radon emanation coefficient in dump-leached uranium tailing sand, J Radioanal Nucl Chem 319(3), 1037 – 1043 (2019),

doi:10.1007/s10967-018-06408-2.

[44] H. Sun and D. J. Furbish, Moisture content effect on radon emanation in porous media, Journal of Contaminant Hydrology 18(3), 239 – 255 (1995), doi:10.1016/0169-7722(95)00002-D.

[45] P. Bossew, The radon emanation power of building materials, soils and rocks, Applied Radiation and Isotopes 59(5 – 6), 389 – 392 (2003), doi:10.1016/j.apradiso.2003.07.001.

[46] R. Ding et al., Study on the pore structure and radon release characteristics of coal in northern China, Science of The Total Environment 844, 157148 (2022), doi:10.1016/j.scitotenv.2022.157148.

[47] Y. Wu et al., A two-dimensional model for the analysis of radon migration in fractured porous media, Environ Sci Pollut Res 30(16), 45966 – 45976 (2023), doi:10.1007/s11356-023-25491-x.

[48] S. Feng et al., Fractal discrete fracture network model for the analysis of radon migration in fractured media, Computers and Geotechnics 128, 103810 (2020), doi:10.1016/j.compgeo.2020.103810.

[49] S. Feng et al., Novel method for measuring temperature-dependent diffusion coefficient of radon in porous media, Applied Radiation and Isotopes 169, 109506 (2021), doi:10.1016/j.apradiso.2020.109506.

[50] C. Xie et al., Temperature-humidity evolution and radon exhalation mechanism of red clay-bentonite covering layer in uranium mill tailings pond, Sci Rep 14(1), 2476 (2024), doi:10.1038/s41598-023-50733-w.

[51] Y. Ye et al., Experimental study on radon exhalation behavior of heap leaching uranium ore column with dilute sulfuric acid, Environ Sci Pollut Res 26(20), 20308 – 20315 (2019), doi:10.1007/s11356-019-05349-x.

[52] D. Huang et al., Identification of sources with abnormal radon exhalation rates based on radon concentrations in underground environments, Science of The Total Environment 807, 150800 (2022), doi:10.1016/j.scitotenv.2021.150800.

[53] N. Wang et al., Experimental studies on the correlation between radon exhalation rate and U/Ra occurrence in sandstone uranium ore, J Radioanal Nucl Chem 334(5), 3335 – 3349 (2025), doi:10.1007/s10967-025-10069-3.

Declaration of Competing Interest

The authors declare that they have no known competing financial interests or personal relationships that could have appeared to influence the work reported in this paper.

Data availability

Data will be made available on request.

Acknowledges

This work was supported by Hunan Provincial Innovation Foundation for Postgraduate (Grant No. CX20251739), Natural Science Foundation of Hunan Province (Grant No.2023JJ50091), Key Projects of Hunan Provincial Department of Education (Grant No.23A0516).